Analyst

Cytokine Analysis at Countable Number of Molecules from Living Single Cell on Nanofluidic Device

Journal:	*Analyst*
Manuscript ID	AN-ART-09-2019-001702.R1
Article Type:	Paper
Date Submitted by the Author:	07-Oct-2019

Complete List of Authors:	Nakao, Tatsuro; The University of Tokyo, School of Engineering Kazoe, Yutaka; The University of Tokyo, Mori, Emi; The University of Tokyo, School of Engineering Morikawa, Kyojiro; The University of Tokyo, School of Engineering Fukasawa, Takemichi; The University of Tokyo Yoshizaki, Ayumi; The University of Tokyo Graduate School of Medicine, Dermatology Kitamori, Takehiko; The University of Tokyo,

Cytokine Analysis at Countable Number of Molecules from Living Single Cell on Nanofluidic Device

Tatsuro Nakao[1], Yutaka Kazoe[2], Emi Mori[2], Kyojiro Morikawa[2] Takemichi Fukasawa[3], Ayumi Yoshizaki[3], and Takehiko Kitamori[1,2*]

[1] Department of Bioengineering, School of Engineering, The University of Tokyo, 7-3-1 Hongo, Bunkyo, Tokyo 113-8656, Japan

[2] Department of Applied Chemistry, School of Engineering, The University of Tokyo, 7-3-1 Hongo, Bunkyo, Tokyo 113-8656, Japan

[3] Department of Dermatology, School of Medicine, The University of Tokyo, 7-3-1 Hongo, Bunkyo, Tokyo 113-8656, Japan

*Correspondence

Dr. Takehiko Kitamori, Department of Applied Chemistry, The University of Tokyo

6A01 Engineering Building No.3, Hongo 7-3-1, Bunkyo, Tokyo 113-0001, Japan

Email: kitamori@icl.t.u-tokyo.ac.jp

Phone: +81-3-5841-7231

Fax: +81-3-5841-6039

Abstract

Analysis of proteins released from living single cell is strongly required in the fields of biology and medicine to elucidate the mechanism of gene expression, cell-cell communication and cytopathology. However, as living single-cell analysis involves fL sample volumes with ultra-small amounts of analyte, comprehensive integration of entire chemical processing for single cell and proteins into spaces smaller than single cell (pL) would be indispensable to prevent dispersion-associated analyte loss. In this study, we proposed and developed a living single-cell protein analysis device based on micro/nanofluidics, and demonstrated analysis of cytokines released from living single B cell by enzyme-linked immunosorbent assay. Based on our integration method and technologies including top-down nanofabrications, surface modifications and pressure-driven flow control, we designed and fabricated the device where pL-microfluidic- and fL-nanofluidic channels are hierarchically allocated for cellular and molecular processing, respectively, and succeeded in micro/nanofluidic control for manipulating single cell and molecules. 13-unit operations for pL-cellular processing including single-cell trapping and stimulation, and fL-molecular processing including fL-volumetry, antigen-antibody reaction and detection were entirely integrated into a microchip. Results suggest analytical performances for countable interleukin (IL)-6 molecules at the limit of detection of 5.27 molecules and that stimulated single B cell secretes 3.41 IL-6 molecules/min. The device is a novel tool for single-cell targeted proteomics, and the methodology of device integration is applicable to other single-cell analyses such as single-cell shotgun proteomics. This study thus provides a general approach and technical breakthroughs that will facilitate further advances in micro/nanofluidics, single-cell life science research, and other fields.

1. Introduction

Single-cell analyses have become increasingly important in studies of the functional heterogeneity on single cells within a genetically homogeneous population.[1, 2] Among these, capability to analyze proteins released from living single cells is now indispensable to the state-of-the-art research examining gene expression, cell-cell communication and cytopathology. For example, B cells, which play a major role in the immune system, are considered to be one of the important etiologies in many autoimmune diseases for which there is still no effective treatment.[3] In fact, B cell ablation therapy has a remarkable therapeutic effect in the clinical field.[4] However, in the B cell population, there are also subpopulations that produce inhibitory cytokines that suppress autoimmunity, and their removal can lead to serious side effects.[5] For this reason, single-cell level identification based on the ability to release cytokines of pathogenic B cells, which are seldom present in patients, is an urgent task.

However, the analysis of proteins secreted by living single cells has been difficult. In contrast to single-cell analyses targeting nucleic acids, for which there are numerous reports,[6-8] single-cell analyses of proteins are challenging. This is primary due to differences in analyte properties: nucleic acids are composed of only 4 kinds of subunits (bases); they are readily amplifiable by polymerase chain reaction; and they are easily separated using techniques such as capillary electrophoresis or hybridization. Proteins, in contrast, are composed of 21 or 22 different subunits (amino acids) with a three-dimensional molecular structure: they are not amplifiable; and their separation requires complex techniques, such as Western blotting or enzyme-linked immunosorbent assay (ELISA). Hence, current single-cell protein analyses are limited to a few approaches even for analysis of cell lysate.[9-11] In addition, analyses of living single cells involve fL (10^{-15} L) sample volumes, which is much smaller than the pL (10^{-12} L) volume of single cell, with ultra-small amounts of analyte protein molecules. Previously, living single-cell protein analyses using nL-μL wells have been reported.[12-14] However, as the volume of analytical field is much larger than fL, the analyte molecules are significantly diluted in the analytical field, causing decrease of sensitivity. Hence, comprehensive integration of entire

chemical processing of single-cell analysis into spaces smaller than single cell (pL) is indispensable to prevent dispersion-associated analyte loss.

On the other hand, microfluidics exploiting 10- to 100 μm microchannels has rapidly developed.[15,16] We have established a general method for integration of chemical processing to realize miniaturized analytical devices.[17] As pL-volume microspaces are similar to the volume of a single cell, microfluidic devices provide advantages in chemical processing of cells.[18,19] Over the last decade, we have extended the field and pioneered nanofluidics exploiting 10- to 1000 nm nanochannels with controlled dimensions.[20] By exploiting fL volumes much smaller than that of a single cell with dominant surface effects, chemical processing of even countable molecules has been realized such as single-molecule ELISA.[21]

Microfluidics and nanofludics provide a potential of enabling analyses of proteins secreted from living single cells by combining cellular and molecular processing in ultra-small volumes; with processing of single cells in pL spaces and protein molecules in fL spaces. However, hybrid integration of microfluidics and nanofluidics has not been achieved. In the present report, we developed a micro/nano-integrated fluidic device for living single-cell protein analysis. A conceptual device design for living single-cell protein analysis based on microfluidics and nanofluidics was proposed. The device was designed to comprehensively integrate chemical processing of single cell and protein molecules, and was fabricated based on top-down glass nanofabrication and bottom-up surface chemical modification. Using the device, analysis of interleukin (IL)-6 secreted from living single B cell was demonstrated.

2. Concept and Design

In this study, the concept for living single-cell protein analysis exploiting microfluidics and nanofluidics was proposed (as illustrated in Figure S1 in Supporting Information). In a conventional analysis of proteins from living cells, the cells are cultured and stimulated in a mL culture dish, the

culture supernatant is sampled using a volumetric pipette, and analyte proteins in the sampled supernatant are quantified by ELISA in μL wells. However, conventional tools employing volumes ranging from μL to mL (much larger than the pL volume of a single cell) are limited to the analysis of 10^4-10^6 cells, which is far from single-cell analysis. Therefore, in our strategy, comprehensive chemical processing of living cell analysis is integrated into micro- and nanochannels hierarchically allocated on a microchip. Chemical processing of a single cell is conducted in the microchannels (pL scale). After sampling the supernatant at a size-interface between micro- and nanochannels, chemical processing of analyte proteins by ELISA is conducted in the nanochannels (fL scale).

Figure 1 illustrates the device design, which was proposed based on methods and technologies developed by our group.[17, 22-24] The device design was based on the integration method known as the micro-unit operation (MUO) and nano-unit operation (NUO).[17] In this method, first a flowchart describing the bulk chemical processing of the analysis is formulated, and then based on a flowchart, bulk chemical processing is broken down into discrete unit operations such as mixing and reaction. Each unit operation is then converted into MUOs or NUOs, and the chemical processing is integrated into the device by connecting these operations in parallel and series. According to this method, a flowchart describing the analyses of living single cell was prepared, and chemical processing was then broken down into 13-unit operations. The unit operations in cellular and molecular processing were converted into MUOs and NUOs respectively, which were connected by a network of micro- and nanochannels composed of a 25 pL-single-cell chamber, a 940 fL-volumetric pipette, a 3.9 pL-flask, an ELISA channel, and branch nanochannels connected to microchannels for injection of reagents. Briefly, (1) a living single cell is selected and captured, and after (2)-(4) stimulation, (5) the supernatant is sampled by fL-volumetry and (6) transported; after (7) dilution, (8), (9) protein molecules contained in the supernatant are separated and (10)-(13) quantified by ELISA. Hydrophilic (silanol), hydrophobic (octadecylsilane), antibody-modified (anti-IL-6 antibody), and blocking (polyethylene glycol) surfaces were incorporated into the channels to realize the functions of each MUO and NUO. The movement

of liquids within the channels is driven by external pressure,[22] with nine pumps installed to control nine reagents. By controlling the balance of pressure, liquid can be driven in the desired direction (see Supplementary Information for details). Liquid-air interfaces are inserted into the channels as necessary to prevent sample dispersion and unintended mixing of reagents via mutual diffusion. The liquid-air interfaces are regulated using a Laplace valves that take advantages of wetting on a hydrophobic surface[23] (see Supplementary Information for details). Detection of non-fluorescent molecules in the nanochannels is achieved using an ultra-high sensitivity photothermal method known as differential interference contrast-thermal lens microscopy (DIC-TLM).[24] An animation demonstrating the operation of the designed device is shown in video S1.

3. Experimental

3.1. Materials

For protein analysis of living single cells, Raji cells were used as model B cells. Raji cells were cultured in RPMI 1640 medium (Thermo Fisher Scientific, MA, USA) supplemented with, 10 %(v/v) fetal bovine serum (FBS), and 1× antibiotic-antimycotic (Thermo Fisher Scientific, MA, USA). Immediately prior to the experiment, the cells were centrifuged, and the pellet was resuspended in fresh culture medium at density of 2×10^6 cells/mL. The stimulation buffer consisted of RPMI 1640 medium, 10 %(v/v) FBS, 1× antibiotic-antimycotic, 40 ng/mL phorbol 12-myristate 13-acetate, and 4 μg/mL ionomycin. MAB206-500 anti-IL-6 antibody (clone 6708, R&D Systems, Inc., Minneapolis, MN, USA) was used for capture in the ELISA channel. The composition of the wash buffer was 100 μM xylene-cyanol, 2%(wt/wt) bovine serum albumin (BSA), 0.05% Tween 20, and 10 mM phosphate buffered saline (PBS). Xylene cyanol, a blue-colored dye, was used for DIC-TLM calibration. The HRP-conjugated antibody solution consisted of 1.5 μg/mL (10 nM) HRP-conjugated anti-IL-6 polyclonal antibody (Abcam, Cambridge, UK) in buffer consisting of 2%(wt/wt) BSA, 0.05% Tween 20, and 10 mM PBS.

3.2. Device Fabrication

Micro- and nanochannels contained in the micro/nano-integrated fluidic device was fabricated using a top-down glass nanofabrication method.[22] Nanochannels were fabricated on a fused-silica substrate of 0.17 mm thickness (VIOSIL, Shin-Etsu Quarts Co., Ltd., Tokyo, Japan) by electron beam lithography using an ELS-7500 system (Elionix, Tokyo, Japan) and plasma etching using an NLD-570 system (ULVAC Co., Ltd., Kanagawa, Japan). The width and depth of the nanochannels were measured by a scanning electron microscopy and a nanoscale optical profiler (WYKO NT9100A, Bruker Corp., MA, USA), respectively. Microchannels with inlet and outlet holes were fabricated on another glass substrate of a 0.7 mm thickness.

After fabricating the micro- and nanochannels on glass substrates, 4 different functional surfaces (designed as shown in Figure 1) were incorporated by partial surface chemical modification methods based on combination of optical patterning and low-temperature bonding of substrates[25, 26] and flowing liquid reagents in channels[27] (details are described in the Supplementary Information). Briefly, the surface of the ELISA channel was modified by capture antibodies via covalent bonding with amino groups modified onto the glass surface. To prevent non-specific adsorption, the nanochannel surface was coated by polyethylene glycol and bovine serum albumin for blocking. For fluid operations utilizing the liquid-air interfaces, the surfaces of fL-volumetric pipette and a microchannel were rendered hydrophobic by modification with octadecylsilane, and the surfaces of a single-cell chamber was rendered hydrophilic by silanol groups.

3.3. Experimental Setup

Figure 2 shows the experimental setup for living single-cell protein analysis. This setup consisted of 3 components: a cell manipulation system, a molecular processing system and a detection system. The cell manipulation system consisted of a pressure controller (MFCS-EZ, Fluigent, Paris, France), optical tweezers (1064 nm, 50 mW under the objective lens, Shigma Koki, Tokyo, Japan) and fluorescence microscope (IX-71, Olympus, Tokyo, Japan). The molecular processing system consisted

of a fluorescence microscope and pressure controllers. The detection system was a DIC-TLM system (excitation at 660 nm, 20 mW. Probing at 532 nm, 1.5 mW). The external pressure for driving liquid movement was determined considering the fluidic resistance of each channels based on the information on fabricated channel sizes (see Tables S1 and S2).

4. Results and Discussion

4.1. Fabricated Device and Confirmation of Surface Modification

Figure 3(a) shows photographs of the device. We successfully fabricated the device as designed. To confirm the surface patterning, pure water was introduced into the nanochannels by capillary filling. Capillary filling is a phenomenon by which water can be introduced into a hydrophilic narrow channel via surface effects without application of external pressure. When we applied this technique to nanochannels, the area of the hydrophilic surface can be estimated from the position of the water. Figure 3(b) left shows the result of capillary filling when pure water was introduced from the stimulation channel without external pressure. As the water/air interface was stabilized at the edge of the single-cell chamber and at the half-way point of the nanochannel between the single-cell chamber and fL-volumetric pipette, the surface patterning of OH/ODS was confirmed. Figure 3(b) right shows the result of capillary filling when pure water was introduced into nanochannels without external pressure. As the water/air interface was stabilized in the nanochannel close (~80 μm) to the pL-flask, the surface patterning of ODS/ PEG was confirmed. Accordingly, we verified the proper surface modifications of the micro/nano-integrated fluidic device.

4.2. Device Operation

Figure 4 shows schematic illustrations and microscopic images of micro/nanofluidic operations for living single-cell protein analysis. Using the fabricated device, analysis of IL-6 secreted from a living single B cell was demonstrated according to the unit operations listed in Figure 1, as described below.

pL-cellular processing: (1) Cell selection: A suspension of 2×10^6 Raji cells/ mL (model B cell)

was introduced into the microchannel. Considering the volume of the microchannel (~200 nL), approximately 400 cells were introduced into the channel. The flow was then stopped and a single Raji cell was selected and transported to the single-cell chamber using optical tweezers (Figure 4(a)). (2) Stimulation: The single cell was stimulated using 40 ng/mL PMA and 4 μg/mL ionomycin introduced into the single-cell chamber (Figure 4(b)). While introducing the stimulant, the cell was held in position using the optical tweezers to prevent it being streamed off. (3) Isolation and (4) incubation: To isolate the single cell suspended in the stimulant from other cells in the microchannel, air was injected to the microchannel to form a gas/liquid interface at the inlet of the single-cell chamber (Figure 4(c)). The isolated living single cell was incubated in the stimulant for 6 h.

fL-molecular processing: (5) Volumetry: External pressure lower than the Laplace pressure at 140 kPa was applied to move the supernatant to fL-volumetric pipette, and a volume of 957 fL was measured (Figure 4(d)). The difference in sampling volume relative to the designed volume (940 fL) was equal to the sample volume accommodated in the narrow part of fL-volumetric pipette. (6) Transfer: By increasing the external pressure higher than 140 kPa, the sample was transferred into pL-flask (Figure 4(e)). (7) Dilution: As the sample in the pL-flask was highly viscous, it was diluted with wash buffer. From the volume of the pL-flask of 3.9 pL, the sample was diluted ~4-fold (Figure 4(f)). (8) Antigen (Ag)-antibody (Ab) reaction: To conduct chemical processing of ELISA, the diluted sample in the pL-flask was transported to the ELISA channel via air pressure. In order to allow sufficient enough time for the Ag-Ab reaction, the air/liquid interface was maintained along the left-side edge of the Ab-immobilized region for 2 min (Figure 4(g)). In (9) B/F separation, washing buffer was introduced into the ELISA channel. To prevent unintended mixing by mutual diffusion between the cell sample and wash buffer, the gas/liquid interface was maintained at a position between the fL-volumetric pipette and pL-flask, as shown in Figure 4(h). Similarly, in (10) Ag-Ab reaction and (11)B/F separation, horseradish peroxidase (HRP)-conjugated Ab solution and wash buffer were introduced into the ELISA channel. In (12) enzymatic reaction, a substrate solution (3,3',5,5'-

tetramethylbenzidine [TMB]) was introduced into the ELISA channel, and the flow was stopped for 60 s to allow for formation of the colored substrate. In (13) detection, the flow was restarted, and the accumulated colored substrate flowing through the nanochannel was detected by DIC-TLM. The resulting DIC-TLM signal as function of time is shown in Figure 6(b).

Finally, all 13- of the unit operations listed in Figure 1 were successfully integrated and carried out. Therefore, our strategy for device design based on pressure-driven flow control proposed in this study provides a guideline of realizing micro/nanofluidic device integrating various chemical operations .

4.3. Calibration Curve for ELISA in Nanochannel

To determine the amount of IL-6 present in the fL-supernatant based on the DIC-TLM signal, a calibrate curve between the number of IL-6 molecules and the signal is necessary. For the calibration experiments, using the ELISA channel repeatedly was a subject. Therefore, we developed a method of repeatable use of ELISA channel by removing the captured IL-6 and HRP-conjugated antibody remaining the capture antibody on the surface. This was done by washing the ELISA channel with a glycine hydrochloric acid solution (pH 2.0) to disrupt antibody binding without affecting the covalent bond between the capture antibody and amino groups on the surface. We verified the repeatable use for the IL-6 analysis with low coefficient of variation of 5.8% (details will be reported elsewhere). Using this procedure, DIC-TLM signals for standard solutions were obtained as shown in Figure 5. In the signal analysis (1000 pM as an example as shown in Figure 5), the time-window corresponding to the region of the capture antibody in the ELISA channel was determined from a flow velocity of 123 μm/s, the position of the DIC-TLM detector, and variation in the arrival time of a reproducible signal peak. If the peak arrival time was inside the window, the signal was regarded as a specific signal from the captured IL-6. If it was outside the window, the signal was regarded as an artifact caused by non-specific adsorption of HRP-labeled antibody.

The relationship between the number of IL-6 molecules and the specific signal derived from

captured IL-6 was then plotted and found to approximate a sigmoid function, as shown in Figure 6(a). The limit of detection (LOD), defined using the signal noise at blank (2σ), and the limit of quantification (LOQ), defined based on the variation of the calibration curve (2σ), were 5.27 and 63.2 molecules, respectively, which verified analytical performance of the device for a countable number of protein molecules.

4.4. Determination of IL-6 Secreted from Living Single B Cell

Figure 6 shows determination of the number of IL-6 molecules included in a fL sample of supernatant from a living single B cell using the calibration curve. In the fL sample, 183 IL-6 molecules were found to be contained under stimulation conditions, whereas 87.6 IL-6 molecules were detected in the absence of stimulation (control). Considering the volumes of the sampling and single-cell chamber, these results indicate that the living single B cell stimulated for 6 hours secretes 3.09×10^3 IL-6 molecules, whereas the unstimulated cell secretes 1.86×10^3 IL-6 molecules over the same time period. Assuming a constant secretion rate in 6-hour incubation, these results suggest that stimulated living single B cell additionally secreted 3.41 IL-6 molecules/min. The estimated secretion rate under the stimulated condition determined using the device in the present study is comparable to that determined from bulk experiments of IL-6 secretion by B cells.[28,29] Therefore, the micro/nano-integrated fluidic device described here achieved the analysis of countable number of protein molecules secreted by a living single cell and is a novel tool for single-cell targeted proteomics.

Accordingly, we integrated entire chemical processing of the living single-cell protein analysis into the micro/nano-integrated fluidic device. Utilizing ultra-small spaces with volumes on the fL to pL scale, quantification of a countable number of cytokine molecules released from a living single B cell was demonstrated. The living single-cell protein analysis device developed in this study has 10^2-times higher sensitivity than other reported approaches exploiting nL-μL wells with LOQ of 10^3-10^4 molecules.[12-14] Thus, the developed device can be a powerful tool for single-cell targeted proteomics. Surprisingly, IL-6 molecules were detected even in control experiment without stimulation. This result

can also be attributed to the 10^2-times higher detection sensitivity of the developed device. In future work, other control experiments such as analyses of genetically modified cell, in which the gene coding for IL-6 is knocked out, will be performed. Such ultra-highly sensitive single-cell protein analyses with the capability to quantify low-copy-number proteins allows clear discrimination between pathogenic and non-pathogenic B cells, and could lead to reliable identification of a therapeutic target.

In addition, based on the obtained result, the time-course living single-cell protein analysis at the time scale of 6 hours is potentially feasible. It is important for the elucidation of the mechanism of cell differentiation[30] and cell-level regulation of circadian rhythm.[31]

The present study is the proof-of-concept for analysis of single-cell protein analysis based on micro/nanofluidics. Currently, technical improvement of the system is ongoing including optimization of the device design and implementation of an open/close valve of nanochannel recently reported by our group.[32] Utilizing an improved analytical system, investigation of cell heterogeneity will be reported in future work.

For engineering aspects, this study is the first achievement of micro/nanofluidic hybrid integration of over 10-unit operations in a femtoliter to picoliter size scale. The device integration shown here is also applicable to other single-cell analyses. For example, integration of fL-scale chromatography exploiting nanochannel as a separation column[33] into the device would enable single-cell shotgun proteomics analysis. Our study provided a general approach and technical breakthroughs that are expected to facilitate further advances in micro/nanofluidics, single-cell life science, and other fields.

5. Conclusions

In this study, we developed a living single-cell protein analysis device based on micro/nanofluidics as a novel platform for single-cell targeted proteomics. A concept of the device in which microchannels for pL-cellular processing and nanochannels for fL-molecular processing are fabricated hierarchically was proposed. Based on our integration method of MUO/NUO, the device was designed to entirely

integrate 13-unit operations in chemical processing for single cell and molecules, and was successfully fabricated based on top-down glass nanofabrication and bottom-up surface chemical modification technologies. Combining the surface chemical modification technologies by optical patterning and flowing liquid reagents into channels, partial surface modification was achieved to incorporate hydrophilic, hydrophobic, antibody-modified, and blocking surfaces into the channels. Using the device, analysis of IL-6 secreted from living single B cell was demonstrated. Based on pressure-driven fluidic control, the 13-unit operations were successfully carried out as designed. The results suggested analytical performances for countable molecules with LOD of 5.27 and LOQ of 63.2 molecules, and revealed that stimulated single B cell secretes 3.41 IL-6 molecules/min. The device is a novel tool for single-cell targeted proteomics, and the methodology of device integration is applicable to other single-cell analyses such as single-cell shotgun proteomics. This study provides a general approach and technical breakthroughs that will facilitate further advances in micro/nanofluidics, single-cell life science research, and other fields.

Conflicts of interest

There are no conflicts of interest to declare.

Acknowledgements

The authors would like to thank Dr. Hisashi Shimizu from The University of Tokyo for making an animation demonstrating the device operation. Fabrication facilities were provided in part by the Academic Consortium for Nano and Micro Fabrication of four universities (The University of Tokyo, Tokyo Institute of Technology, Keio University and Waseda University, JAPAN). The authors gratefully acknowledge financial support from Grant-in-Aid for JSPS Fellows 17J10031 and Core Research for Evolutional Science and Technology (CREST) of the Japan Science and Technology Agency (JST): JPMJCR14G1.

References

1 P.K. Chattopadhyay, T.M. Gierahn, M. Roederer and J.C. Love, *Nat. Immunol.*, 2014, **15**, 128-135.

2 P.S. Hoppe, D.L. Coutu and T. Schroeder, *Nature Cell Biology*, 2014, **16**, 919-927.

3 S. Ma, C. Wang, X. Mao and Y. Hao, *Front. Immunol.*, 2019, **10**, 318.

4 T.A. Barr, P. Shen, S. Brown, V. Lampropoulou, T. Roch, S. Lawrie, B. Fan, R.A. O'Connor, S.M. Anderton, A. Bar-Or, S. Fillatreau and D. Gray, *J. Exp. Med.*, 2012, **209**, 1001-1010.

5 A. Yoshizaki, T. Miyagaki, D.J. DiLillo, T. Matsushita, M. Horikawa, E.I. Kountikov, R. Spolski, J.C. Poe, W.J. Leonard and T.F. Tedder, *Nature*, 2012, **491**, 264-268.

6 A. Shalek, R. Satija, X. Adiconis, R. Gertner, J. Gaublomme, R. Raychowdhury, S. Schwartz, N. Yosef, C. Malboeuf, D. Lu, J. Trombetta, D. Gennert, A. Gnirke, A. Goren, N. Hacohen, J. Levin and H. Park, A. Regev, *Nature*, 2013, **498**, 236-240.

7 E. Shapiro, T. Biezuner and S. Linnarsson, *Nature Reviews Genetics*, 2013, **14**, 618-630.

8 S.S. Potter, *Nature Reviews Nephrology,* 2018, **14**, 479-492.

9 C. Albayrak, C.A. Jordi, C. Zechner, J. Lin, C.A. Bichsel, M. Khammash and S. Tay, *Mol. Cell*, 2016, **61**, 914-924.

10 K. Eyer, P. Kuhn, C. Hanke and P.S. Dittrich, *Lab Chip*, 2012, **12**, 765-772.

11 A.J. Hughes, D.P. Spelke, Z. Xu, C.-C. Kang, D.V. Schaffer and A.E. Herr, *Nat. Methods*, 2014, **11**, 749-755.

12 A. Tarkowski, C. Czerkinsky, L.Å. Nilsson, H. Nygren and Ö. Ouchterlony, *J. Immunol. Methods*, 1984, **72**, 451-459.

13 C. Ma, R. Fan, H. Ahmad, Q. Shi, B. Comin-Anduix, T. Chodon, R.C. Koya, C.-C. Liu, G.A. Kwong, C.G. Radu, A. Ribas and J.R. Heath, *Nat. Med.*, 2011, **17**, 738-743.

14 A.J. Torres, A.S. Hill and J.C. Love, *Anal. Chem.*, 2014, **86**, 11562-11569.

15 E.K. Sackmann, A.L. Fulton and D.J. Beebe, *Nature*, 2014, **507**, 181-189.

16 T.A. Duncombe, A.M. Tentori and A.E. Herr, *Nat. Rev. Mol. Cell Biol.*, 2015, **16**, 554-567.

17 M. Tokeshi, T. Minagawa, K. Uchiyama, A. Hibara, K. Sato, H. Hisamoto and T. Kitamori, *Anal. Chem.*, 2002, **74**, 1565-1571.

18 H. Yun, K. Kim and W.G. Lee, *Biofabrication*, 2013, **5**, 022001.

19 J. Sibbitts, K.A. Sellens, S. Jia, S.A. Klasner and C.T. Culbertson, *Anal. Chem.*, 2018, **90**, 65-85.

20 A. Hibara, T. Saito, H.-B. Kim, M. Tokeshi, T. Ooi, M. Nakao and T. Kitamori, *Anal. Chem.*, 2002, **74**, 6170-6176.

21 K. Shirai, K. Mawatari, R. Ohta, H. Shimizu and T. Kitamori, *Analyst*, 2018, **143**, 943-948.

22 T. Tsukahara, K. Mawatari, A. Hibara and T. Kitamori, *Anal. Bioanal. Chem.*, 2008, **391**, 2745-2752.

23 G. Takei, M. Nonogi, A. Hibara, T. Kitamori and H.-B. Kim, *Lab Chip*, 2007, **7**, 596-602.

24 H. Shimizu, K. Mawatari and T. Kitamori, *Anal. Chem.*, 2009, **81**, 9802-9806.

25 K. Shirai, K. Mawatari and T. Kitamori, *Small*, 2014, **10**, 1514-1522.

26 Y. Xu, C. Wang, L. Li, N. Matsumoto, K. Jang, Y. Dong, K. Mawatari, T. Suga and T. Kitamori, *Lab Chip*, 2013, **13**, 1048-1052.

27 A. Hibara, S. Iwayama, S. Matsuoka, M. Ueno, Y. Kikutani, M. Tokeshi and T. Kitamori, *Anal. Chem.*, 2005, **77**, 943-947.

28 A.J. Szczepek, A.R. Belch and L.M. Pilarski, *Exp. Hematol.*, 2001, **29**, 1076-1081.

29 M.V. Hobbs, R.J. McEvilly, R.J. Koch, G.J. Cardenas and D.J. Noonan, *Cell. Immunol.*, 1991, **132**, 442-450.

30 P. R. van den Berg, B. Budnik, N. Slavov and S. Semrau, *bioRxiv*, 2017, 1-35.

31 G. Rey, N.B. Milev, U.K. Valekunja, R. Ch, S. Ray, M. Silva Dos Santos, A.D. Nagy, R. Antrobus, J.I. MacRae and A.B. Reddy, *Mol. Syst. Biol.*, 2018, **14**, e8376.

32 Y. Kazoe, Y. Pihosh, H. Takahashi, T. Ohyama, H. Sano, K. Morikawa, K. Mawatari and T.

Kitamori, *Lab Chip*, 2019, **19**, 1686-1694.

33 R. Ishibashi, K. Mawatari, T. Kitamori, *Small*, 2012, **8**, 1237-1242.

Table of Contents Entry

Analysis of coutable number of protein molecules released from living single cell was realized by a micro/nanofluidic device entirely integrating cellular processing and molecular processing into pL-microchannels and fL-nanochannels, respectively.

Figure Captions

Figure 1. Device design based on micro-unit operation (MUO) and nano-unit operation (NUO). Chemical processing for living single-cell protein analysis is broken down into 13-unit operations according to a flowchart, and these operations are converted into 4MUOs and 9 NUOs. These MUOs and NUOs are connected in parallel and series to integrate chemical processing into the device.

Figure 2. Schematic diagram of the experimental setup for living single-cell protein analysis.

Figure 3. Results of fabrication: (a) The device fabricated using a top-down/bottom-up nanofabrication methods. (b) Confirmation of surface patterning by capillary filling with pure water.

Figure 4. Results of micro/nanofluidic operations for living single-cell protein analysis. pL-cellular processing includes (a) 1. single-cell selection, (b) 2. stimulation, (c) 3. Isolation, and 4. incubation. fL-molecular processing includes (d) 5. volumetry, (e) 6. transfer, (f) 7. dilution, (g) 8. Ag-Ab reaction, (h) 9. B/F separation, 10. Ag-Ab reaction, 11. B/F separation, 12. enzymatic reaction and 13. detection.

Figure 5. Calibration experiments: DIC-TLM signals of standard solutions (0-1000 pM IL-6) derived from colored substrate (TMB) as function of time, which were obtained using the ELISA channel repeatedly.

Figure 6. Results of living single-cell protein analysis: (a) Calibration curve of the number of IL-6 molecules in a fL sample versus the area of the signal peak. (b) DIC-TLM signals for a stimulated and unstimulated (control) living single B cell. The number of IL-6 molecules in the fL supernatant sample was estimated using the calibration curve.

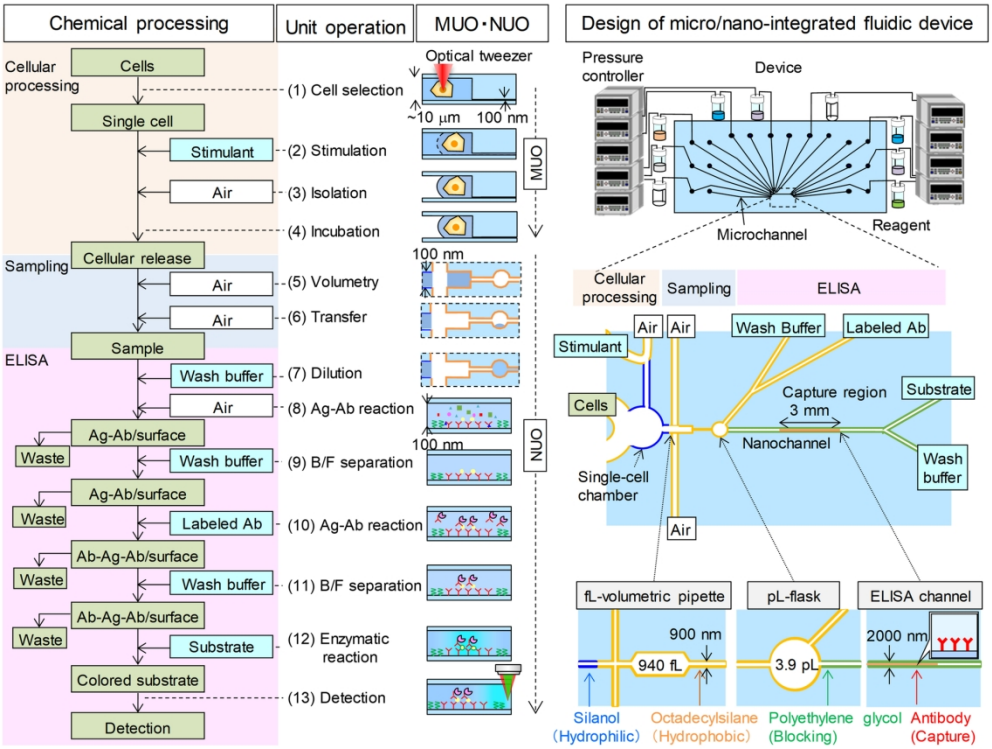

Figure 1

171x127mm (300 x 300 DPI)

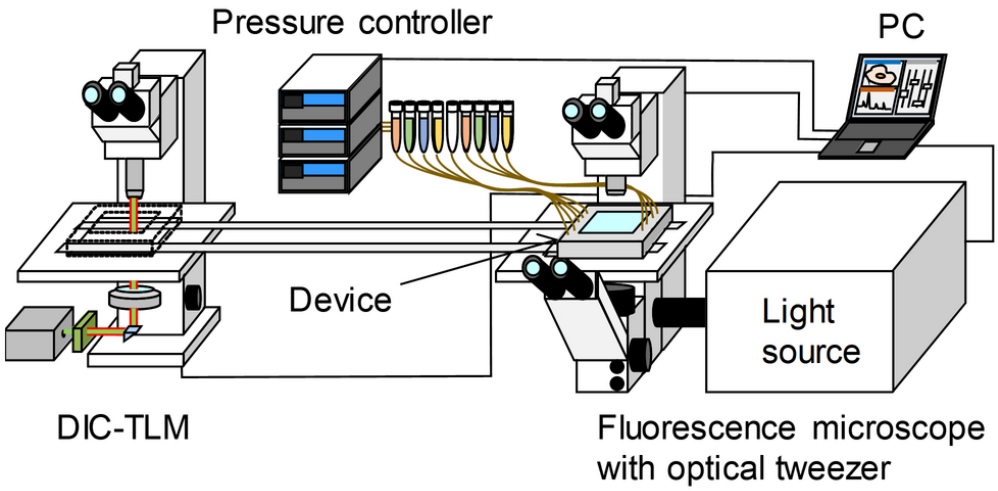

Figure 2

82x43mm (300 x 300 DPI)

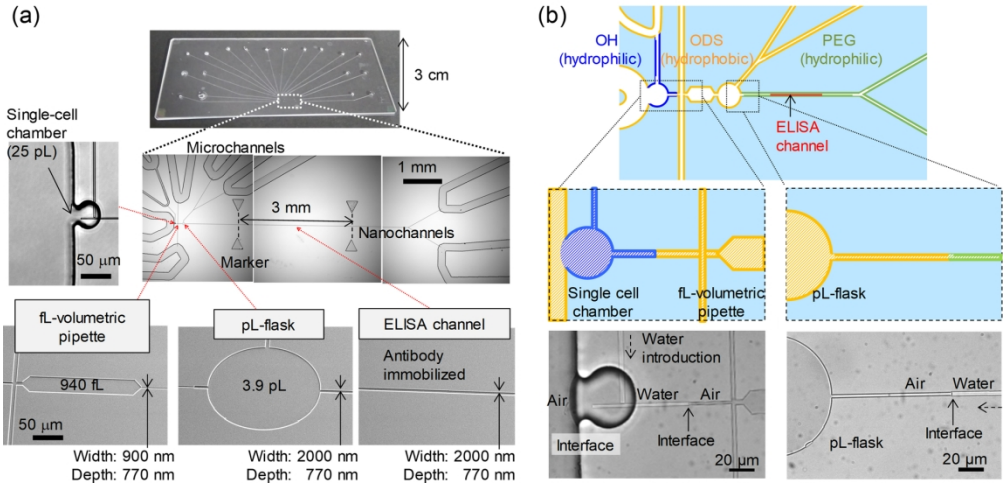

Figure 3

170x82mm (300 x 300 DPI)

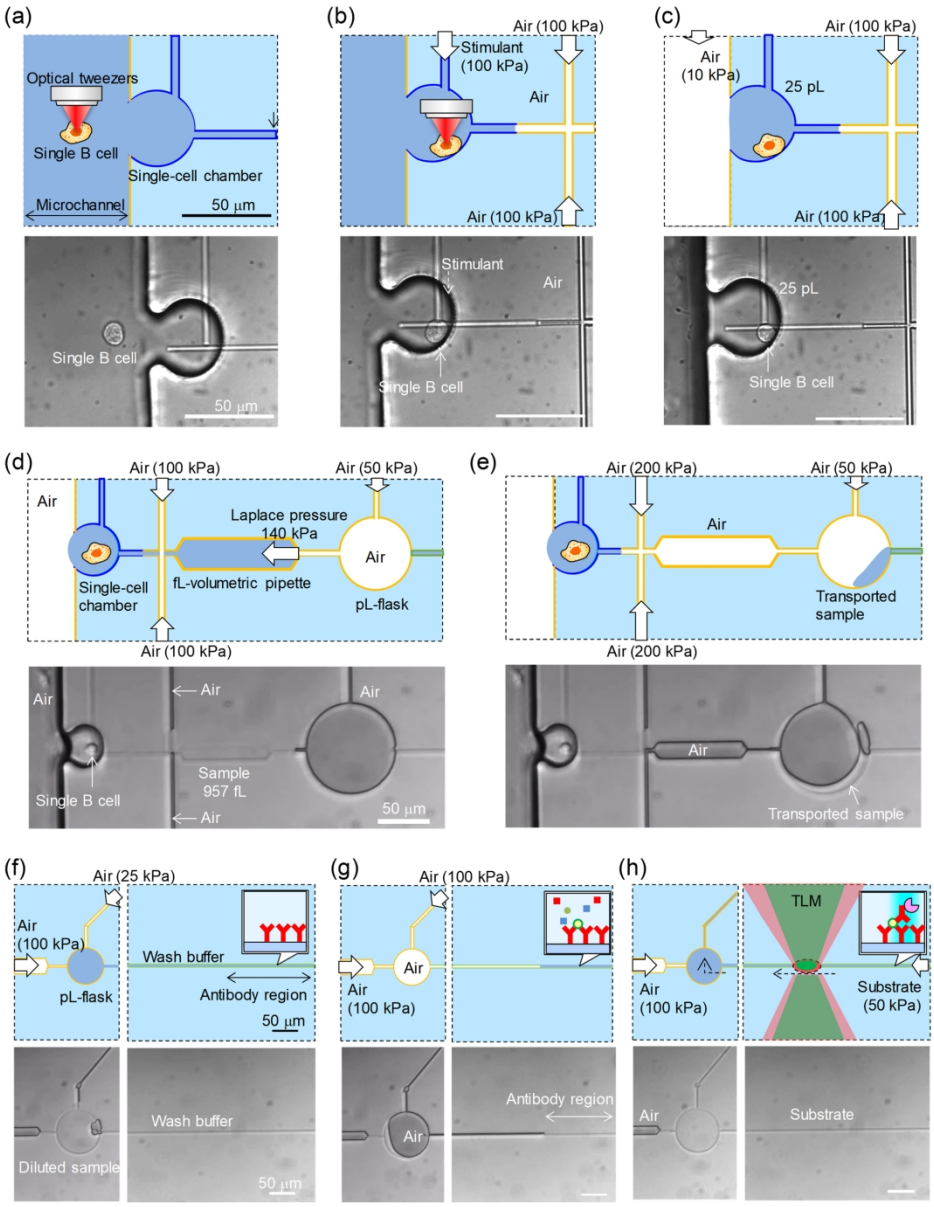

Figure 4

171x219mm (300 x 300 DPI)

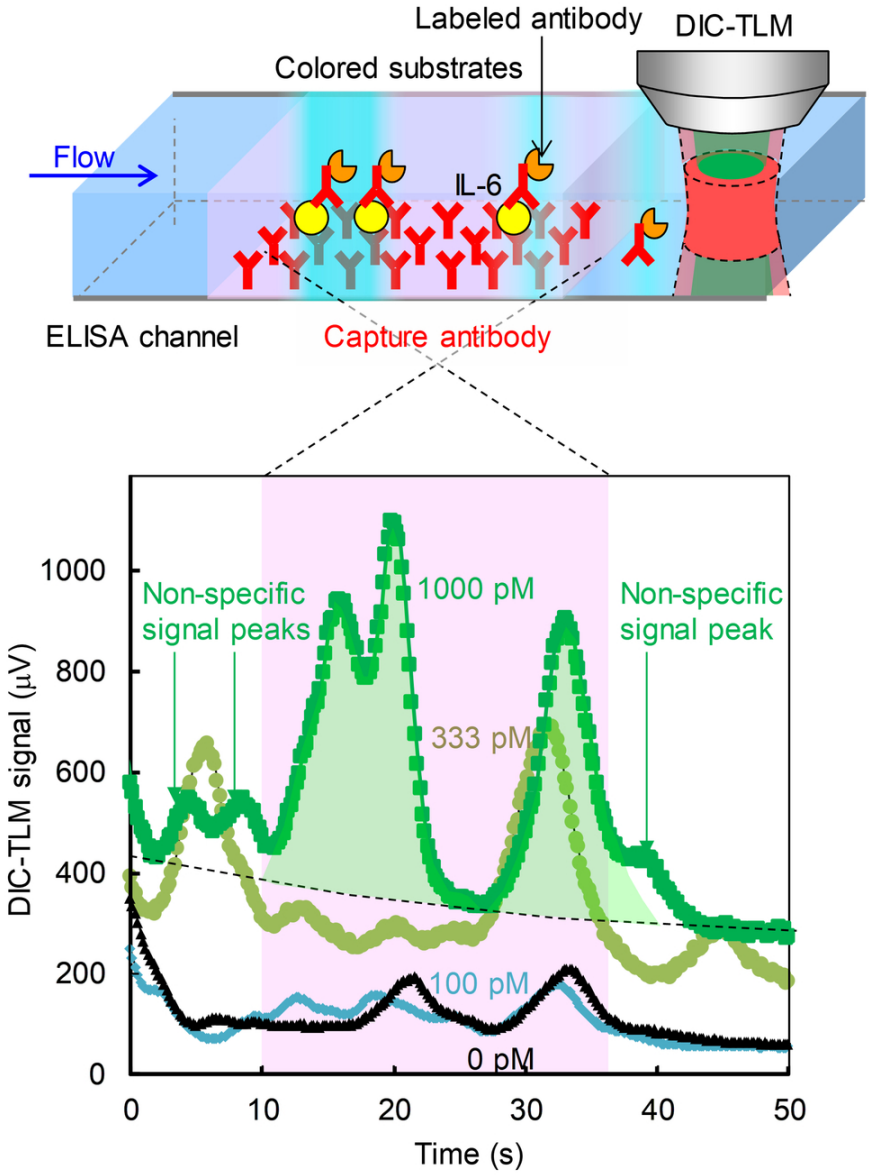

Figure 5

82x112mm (300 x 300 DPI)

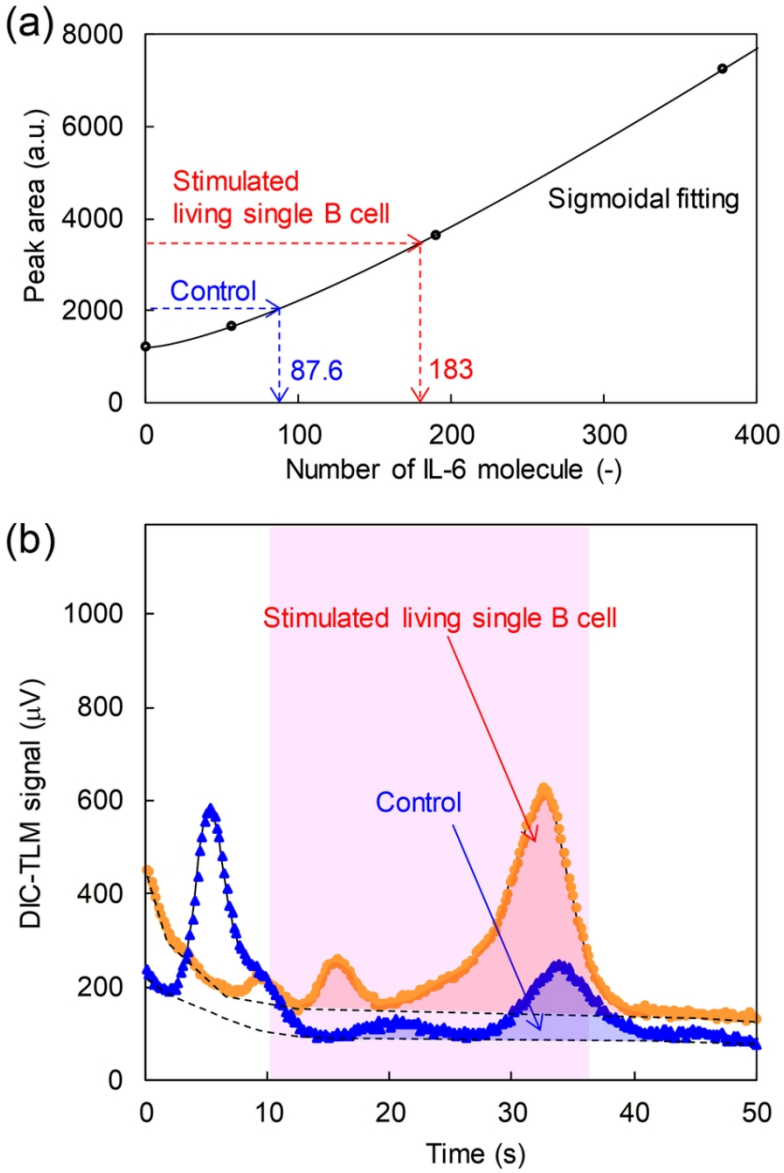

Figure 6

82x123mm (300 x 300 DPI)

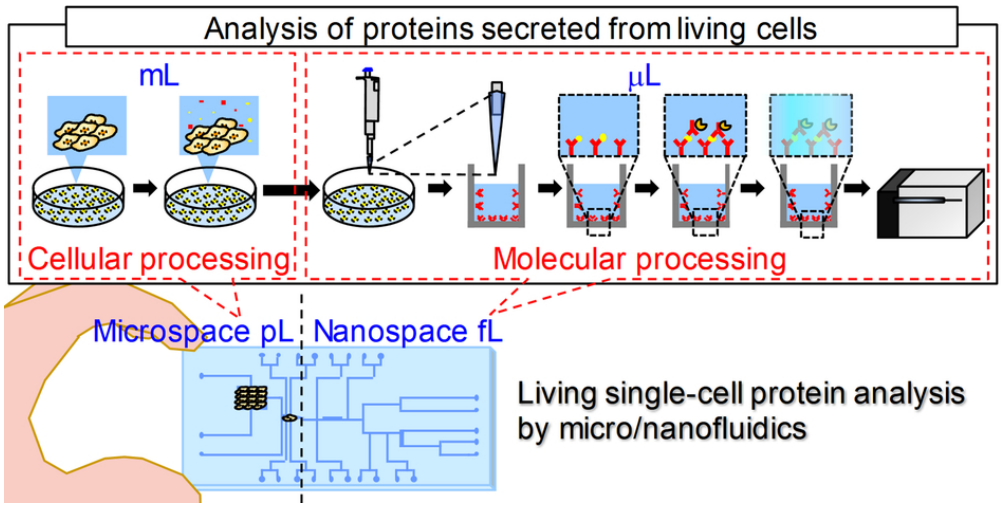

79x39mm (300 x 300 DPI)